Polarization of the vacuum of a quantized scalar field by an impenetrable magnetic vortex of finite thickness

2010 J. Phys. A: Math. Theor. 43 175401

(http://iopscience.iop.org/1751-8121/43/17/175401)

IOP PUBLISHING JOURNAL OF PHYSICS A: MATHEMATICAL AND THEORETICAL

J. Phys. A: Math. Theor. **43** (2010) 175401 (12pp) doi:10.1088/1751-8113/43/17/175401

Polarization of the vacuum of a quantized scalar field by an impenetrable magnetic vortex of finite thickness

V M Gorkavenko[1], Yu A Sitenko[2] and O B Stepanov[1]

[1] Department of Physics, Taras Shevchenko National University of Kyiv, 64 Volodymyrs'ka str., Kyiv 01601, Ukraine
[2] Bogolyubov Institute for Theoretical Physics, National Academy of Sciences of Ukraine, 14-b Metrologichna str., Kyiv 03680, Ukraine

E-mail: gorka@univ.kiev.ua

Received 25 November 2009, in final form 2 March 2010
Published 13 April 2010
Online at stacks.iop.org/JPhysA/43/175401

Abstract
We consider the effect of the magnetic field background in the form of a tube of the finite transverse size on the vacuum of the quantized charged massive scalar field which is subject to the Dirichlet boundary condition at the tube. It is shown that if the Compton wavelength associated with the scalar field considerably exceeds the transverse size of the tube, then the vacuum energy which is finite and periodic in the value of the magnetic flux enclosed in the tube is induced on a plane transverse to the tube. Some consequences for generic features of the vacuum polarization in the cosmic-string background are discussed.

PACS numbers: 11.27.+d, 11.10.Kk, 11.15.Tk

1. Introduction

The emergence of calculable and detectable vacuum energy as a consequence of imposing external boundary conditions in quantum field theory was predicted more than 60 years ago by Casimir [1]. Since then the vacuum energy of fluctuating quantum fields that are subject to boundary conditions has been studied in various setups (see, e.g., reviews in [2–4]). Usually, the boundary manifold is chosen to be noncompact disconnected (e.g. two parallel infinite plates, as generically in [1]) or closed compact (e.g. box or sphere); see [2–4].

In the present paper, we shall consider the boundary manifold which is noncompact connected and has the form of an infinite tube in three-dimensional space. As has been first demonstrated by Aharonov and Bohm [5] in the framework of first-quantized theory, the magnetic flux enclosed in such a tube affects the properties of quantum matter outside the tube. This effect which is named after them has no analogues in classical physics and is characterized by the periodic dependence on the value of the flux, vanishing at integer multiples of the London flux value, while being maximal at half of the London flux value.

In the framework of second-quantized theory, one is interested in the vacuum polarization effects which are induced outside the tube by the magnetic flux enclosed in the tube. In particular, the question is whether the vacuum energy is induced. If this is the case, then this may be denoted as the Casimir–Bohm–Aharonov effect (see also [6]).

It should be noted that initially [5] the Bohm–Aharonov effect was considered under the assumption that the transverse size of the tube is zero, which corresponds to the singular magnetic vortex configuration. Taking into account the finite transverse size of the tube was an important task, since in reality a vortex-forming solenoid is of finite width[3]. This task was fulfilled once before, see [7, 8]. Although, unlike the case of a singular vortex, the quantum-mechanical problem in the case of a finite-thickness vortex is not exactly solvable, a thorough analysis has been carried out, and, in particular, it has been shown that the Bohm–Aharonov effect disappears at a sufficiently large thickness of an impenetrable magnetic vortex [7].

Returning to quantum field theory, and, appropriately, to the Casimir–Bohm–Aharonov effect, we note that up to now this effect was considered for the case of a singular magnetic vortex only [6, 9–11]. Therefore, the aim of the present paper is to make a first step in the study of the dependence on the thickness of an impenetrable magnetic vortex. It should be noted that vacuum polarization effects which are induced by magnetic fluxes of finite thickness were considered by different authors, see [12–16]. However, these authors are concerned with the case when there is no boundary at all and the region of the flux is penetrable for the quantized matter fields; therefore, the obtained results have no relation neither to the Casimir, nor to the Bohm–Aharonov effects. In the present paper we shall show that, similar to the Bohm–Aharonov effect, the Casimir–Bohm–Aharonov effect disappears at a sufficiently large thickness of the vortex. The second-quantized matter will be represented by the charged massive scalar field.

In the next section a general definition of the vacuum energy density for the quantized scalar field is reviewed and a starting expression for its renormalized value is given. In section 3 this value is calculated numerically in the case of $(2+1)$-dimensional space-time. Finally, the results are summarized and discussed in section 4.

2. Vacuum energy density

The operator of the quantized charged scalar field is represented in the form

$$\Psi(x^0, \boldsymbol{x}) = \sum\!\!\!\!\!\!\int_{\lambda} \frac{1}{\sqrt{2E_\lambda}} \left[\mathrm{e}^{-\mathrm{i}E_\lambda x^0} \psi_\lambda(\boldsymbol{x})\, a_\lambda + \mathrm{e}^{\mathrm{i}E_\lambda x^0} \psi_{-\lambda}(\boldsymbol{x})\, b_\lambda^\dagger \right], \tag{1}$$

where $a_\lambda^\dagger$ and a_λ $\left(b_\lambda^\dagger \text{ and } b_\lambda\right)$ are the scalar particle (antiparticle) creation and destruction operators satisfying commutation relations; the wavefunctions $\psi_\lambda(\mathbf{x})$ form a complete set of solutions to the stationary Klein–Gordon equation

$$(-\boldsymbol{\nabla}^2 + m^2)\psi_\lambda(\boldsymbol{x}) = E_\lambda^2 \psi(\boldsymbol{x}), \tag{2}$$

where $\boldsymbol{\nabla}$ is the covariant derivative in an external (background) field and m is the mass of the scalar particle; λ is the set of parameters (quantum numbers) specifying the state; $E_\lambda = E_{-\lambda} > 0$ is the energy of the state; the symbol $\sum\!\!\!\!\!\!\int_{\lambda}$ denotes summation over discrete and integration (with a certain measure) over continuous values of λ.

[3] Also, a real solenoid is of finite length. However, in the case when the width of the solenoid is much smaller than its length and the motion of a quantum-mechanical particle is confined to a plane which is transverse to the solenoid, the effects of the width prevail over the effects of the length.

We are considering the static background in the form of the cylindrically symmetric magnetic vortex of finite thickness; hence, the covariant derivative is $\mathbf{\nabla} = \boldsymbol{\partial} - \mathrm{i}e\boldsymbol{V}$ with the vector potential possessing only one nonvanishing component given by

$$V_\varphi = \Phi/2\pi \tag{3}$$

outside the vortex; here, Φ is the vortex flux and φ is the angle in the polar (r, φ) coordinates on a plane which is transverse to the vortex. The Dirichlet boundary condition on the edge $(r = r_0)$ of the vortex is imposed on the scalar field:

$$\psi_\lambda|_{r=r_0} = 0, \tag{4}$$

i.e. quantum matter is assumed to be perfectly reflected from the thence impenetrable vortex. Provided the orthonormalization condition is satisfied,

$$\int \mathrm{d}^3x\, \psi^*_\lambda \psi_{\lambda'} = \langle\lambda|\lambda'\rangle, \tag{5}$$

the solution to (2) and (4) in the case of the impenetrable magnetic vortex of thickness $2r_0$ takes the form

$$\psi_{knk_z}(\boldsymbol{x}) = (2\pi)^{-1}\,\mathrm{e}^{\mathrm{i}k_z z}\,\mathrm{e}^{\mathrm{i}n\varphi}\beta_n(kr_0) \times [Y_{|n-e\Phi/2\pi|}(kr_0)J_{|n-e\Phi/2\pi|}(kr) - J_{|n-e\Phi/2\pi|}(kr_0)Y_{|n-e\Phi/2\pi|}(kr)], \tag{6}$$

where z is the coordinate along the vortex,

$$\beta_n(kr_0) = \left[Y^2_{|n-e\Phi/2\pi|}(kr_0) + J^2_{|n-e\Phi/2\pi|}(kr_0)\right]^{-1/2}, \tag{7}$$

and $0 < k < \infty$, $-\infty < k_z < \infty$, $n \in \mathbb{Z}$ ($\mathbb{Z}$ is the set of integer numbers); $J_\mu(u)$ and $Y_\mu(u)$ are the Bessel functions of order μ of the first and second kinds. It should be noted that the vortex can be obviously generalized to d-dimensional space by adding extra $d-3$ longitudinal coordinates to z; then factor $(2\pi)^{-1}\,\mathrm{e}^{\mathrm{i}k_z z}$ is changed to $(2\pi)^{\frac{1-d}{2}}\,\mathrm{e}^{\mathrm{i}\boldsymbol{k}_z \boldsymbol{z}}$, where $\boldsymbol{z}$ is the $(d-2)$-dimensional vector which is orthogonal to the (r, φ)-plane in d-dimensional space.

In general, the vacuum energy density is determined as the vacuum expectation value of the time–time component of the energy–momentum tensor, that is given formally by the expression

$$\varepsilon = \langle\mathrm{vac}|(\partial_0\Psi^+\partial_0\Psi + \partial_0\Psi\partial_0\Psi^+)|\mathrm{vac}\rangle = \sum\!\!\!\!\!\!\int_\lambda E_\lambda \psi^*_\lambda(\boldsymbol{x})\,\psi_\lambda(\boldsymbol{x}), \tag{8}$$

which is ill-defined, suffering from the ultraviolet divergencies: the momentum integral corresponding to the last expression in (8) diverges as p^{d+1} for $p \to \infty$. The well-defined quantity is obtained with the use of regularization and then renormalization procedures (see, e.g., [3]). As to regularization, one employs conventionally either heat-kernel or zeta-function methods (see, e.g., [2]). As to renormalization, it has been shown [17] that, for a specific configuration of a vortex through the excluded region, it suffices, irrespective of the number of spatial dimensions, to perform one subtraction, namely to subtract the contribution corresponding to the absence of the vortex. This fact owes to the symmetry in the problem, being of rather general nature. It is consistent, for instance, with a more recent result obtained in a quite different setup in paper [18], where the Casimir energy per unit length for n non-overlapping parallel cylinders of infinite length in three-dimensional space is shown to be directly related (without the need of an extra subtraction or an extra counter-term) to the Casimir energy for n non-overlapping discs in two-dimensional space.

Thus, the renormalized vacuum energy density in the case of the finite-thickness vortex takes the form

$$\varepsilon_{\mathrm{ren}} = (2\pi)^{1-d}\int \mathrm{d}^{d-2}k_z \int_0^\infty \mathrm{d}k\, k\left(\boldsymbol{k}_z^2 + k^2 + m^2\right)^{1/2}[S(kr, kr_0) - S(kr, kr_0)|_{\Phi=0}], \tag{9}$$

where, in view of (6),

$$S(kr, kr_0) = \sum_{n\in\mathbb{Z}} \beta_n^2(kr_0)[Y_{|n-e\Phi/2\pi|}(kr_0)J_{|n-e\Phi/2\pi|}(kr) - J_{|n-e\Phi/2\pi|}(kr_0)Y_{|n-e\Phi/2\pi|}(kr)]^2. \tag{10}$$

Owing to the infinite range of summation, the last expression is periodic in the flux Φ with period equal to $2\pi e^{-1}$, i.e. it depends on the quantity

$$F = \frac{e\Phi}{2\pi} - \left[\left[\frac{e\Phi}{2\pi}\right]\right], \tag{11}$$

where $[[u]]$ is the integer part of quantity u (i.e. the integer which is less than or equal to u).

Let us rewrite (10) in the form

$$S(kr, kr_0) = S_0(kr) + S_1(kr, kr_0), \tag{12}$$

where $S_0(kr)$ corresponds to the appropriate series in the case of the vacuum polarization by a singular magnetic vortex [9–11]:

$$S_0(kr) = \sum_{n=0}^{\infty}\left[J_{n+F}^2(kr) + J_{n+1-F}^2(kr)\right] = \int_0^{kr} \mathrm{d}\tau[J_F(\tau)J_{-1+F}(\tau) + J_{-F}(\tau)J_{1-F}(\tau)], \tag{13}$$

and $S_1(kr, kr_0)$ is a correction term due to the finite thickness of a vortex:

$$\begin{aligned} S_1(kr, kr_0) = 2\sum_{n=0}^{\infty}\Bigg[& J_{n+F}(kr_0)Y_{n+F}(kr)\frac{J_{n+F}(kr_0)Y_{n+F}(kr) - Y_{n+F}(kr_0)J_{n+F}(kr)}{J_{n+F}^2(kr_0) + Y_{n+F}^2(kr_0)} \\ & + J_{n+1-F}(kr_0)Y_{n+1-F}(kr)\frac{J_{n+1-F}(kr_0)Y_{n+1-F}(kr) - Y_{n+1-F}(kr_0)J_{n+1-F}(kr)}{J_{n+1-F}^2(kr_0) + Y_{n+1-F}^2(kr_0)}\Bigg] \\ & - \sum_{n=0}^{\infty}\Bigg[J_{n+F}^2(kr_0)\frac{J_{n+F}^2(kr) + Y_{n+F}^2(kr)}{J_{n+F}^2(kr_0) + Y_{n+F}^2(kr_0)} \\ & + J_{n+1-F}^2(kr_0)\frac{J_{n+1-F}^2(kr) + Y_{n+1-F}^2(kr)}{J_{n+1-F}^2(kr_0) + Y_{n+1-F}^2(kr_0)}\Bigg]. \end{aligned} \tag{14}$$

In the absence of the magnetic flux in the tube we have

$$S(kr, kr_0)|_{\Phi=0} = \tilde{S}_0 + \tilde{S}_1(kr, kr_0), \tag{15}$$

where

$$\tilde{S}_0 = J_0^2(kr) + 2\sum_{n=1}^{\infty} J_n^2(kr) = 1, \tag{16}$$

and a correction term due to the finite thickness of an empty tube:

$$\begin{aligned} \tilde{S}_1(kr, kr_0) = 2\Bigg[& J_0(kr_0)Y_0(kr)\frac{J_0(kr_0)Y_0(kr) - Y_0(kr_0)J_0(kr)}{J_0^2(kr_0) + Y_0^2(kr_0)} \\ & + 2\sum_{n=1}^{\infty} J_n(kr_0)Y_n(kr)\frac{J_n(kr_0)Y_n(kr) - Y_n(kr_0)J_n(kr)}{J_n^2(kr_0) + Y_n^2(kr_0)}\Bigg] \\ & - \Bigg[J_0^2(kr_0)\frac{J_0^2(kr) + Y_0^2(kr)}{J_0^2(kr_0) + Y_0^2(kr_0)} + 2\sum_{n=1}^{\infty} J_n^2(kr_0)\frac{J_n^2(kr) + Y_n^2(kr)}{J_n^2(kr_0) + Y_n^2(kr_0)}\Bigg]. \end{aligned} \tag{17}$$

Thus, vacuum energy density (9) depends on F (11), i.e. it is periodic in the flux Φ with a period equal to $2\pi e^{-1}$. Moreover, relation (9) is symmetric under the substitution $F \to 1 - F$,

vanishing at $F \to 0$ ($F \to 1$) and, perhaps, attaining its maximal value at $F = 1/2$.[4] Relations (13) and (14) are simplified at $F = 1/2$:

$$S_0(kr)|_{\Phi=\pi e^{-1}} = \frac{2}{\pi}\int_0^{2kr} \frac{\mathrm{d}\tau}{\tau}\sin\tau, \tag{18}$$

and

$$S_1(kr, kr_0)|_{\Phi=\pi e^{-1}} = 2\sum_{n=0}^{\infty} \frac{J^2_{n+\frac{1}{2}}(kr_0)\left[Y^2_{n+\frac{1}{2}}(kr) - J^2_{n+\frac{1}{2}}(kr)\right] - 2J_{n+\frac{1}{2}}(kr_0)Y_{n+\frac{1}{2}}(kr_0)J_{n+\frac{1}{2}}(kr)Y_{n+\frac{1}{2}}(kr)}{J^2_{n+\frac{1}{2}}(kr_0) + Y^2_{n+\frac{1}{2}}(kr_0)}. \tag{19}$$

Since it is hardly possible to evaluate sums in (14) and (17) analytically, our further analysis will employ numerical calculation. In the following we restrict ourselves to the case of $F = 1/2$ and $d = 2$, when the expression for the vacuum energy density takes the form

$$\varepsilon_{\mathrm{ren}} = \frac{1}{2\pi}\int_0^{\infty} \mathrm{d}k\, k(k^2 + m^2)^{1/2} G(kr, kr_0), \tag{20}$$

where

$$G(kr, kr_0) = S(kr, kr_0)|_{\Phi=\pi e^{-1}} - S(kr, kr_0)|_{\Phi=0}. \tag{21}$$

3. Numerical evaluation of the vacuum energy density

We rewrite (20) in the dimensionless form

$$r^3\varepsilon_{\mathrm{ren}} = \frac{1}{2\pi}\int_0^{\infty} \mathrm{d}z\, z\sqrt{z^2 + \left(\frac{mr_0}{\lambda}\right)^2}\, G(z, \lambda z), \tag{22}$$

where $\lambda = r_0/r$, $\lambda \in [0, 1]$. Let us point out some analytical properties of the integrand function in (22): it vanishes at the edge of the vortex

$$\lim_{\lambda\to 1} G(z, \lambda z) = 0; \tag{23}$$

at large distances from the vortex the case of a singular vortex is recovered:

$$\lim_{\lambda\to 0} G(z, \lambda z) = S_0(z)|_{\Phi=\pi e^{-1}} - \tilde{S}_0; \tag{24}$$

at small values of z one gets

$$G(z, \lambda z)|_{z\to 0} = -[\ln(\lambda)/\ln(\lambda z)]^2. \tag{25}$$

Numerical analysis indicates that in the calculation of the function $G(z, \lambda z)$ one can use series in (17) and (19) with finite limits, namely for calculating $G(z, \lambda z)$ at point $z = z'$ it is enough to cut off the summation limits by $n = [[z' + 30]]$. In this case the relative error is

$$\left|\frac{G(z, \lambda z)|_{n\in(0,[[z+30]])} - G(z, \lambda z)}{G(z, \lambda z)}\right| < \delta(\lambda), \qquad \delta(\lambda) < 10^{-17}, \qquad \lambda \in [1/10, 9/10]. \tag{26}$$

It can be shown that the envelope of $G(z, \lambda z)$ is an exponentially decreasing function at large z, see figure 1. So, for the finite-thickness magnetic vortex we can compute values of the

[4] At least, this is certainly true in the case of the singular vortex both for the Bohm–Aharonov [5] and the Casimir–Bohm–Aharonov [6, 9–11] effects.

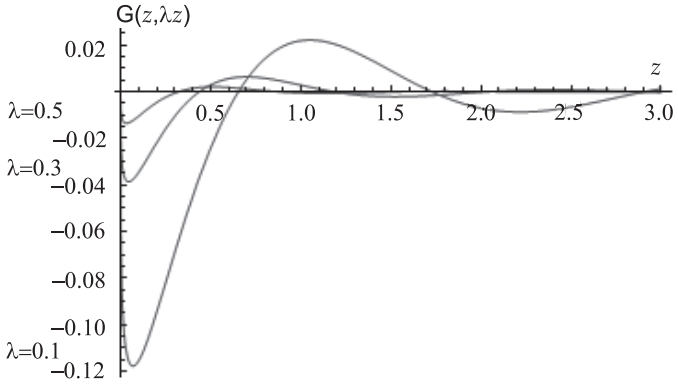

Figure 1. Behaviour of $G(z, \lambda z)$ at different values of λ.

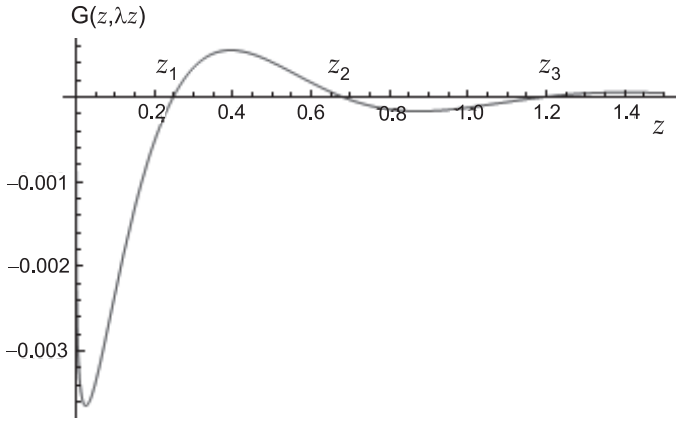

Figure 2. The location of roots of $G(z, \lambda z)$ at $\lambda = 0.7$.

dimensionless quantity $r^3\varepsilon_{\text{ren}}$ (22) for different (not very small) values of λ. To do this, we have to be able to perform integration in (22) with high precision. This is carried out in the following way.

As one can see from figure 2, the function $G(z, \lambda z)$ is negative from $z = 0$ to the first function root at $z = z_1$ ($z_1 \neq 0$). So, the appropriate integral in (22) is negative. The subsequent roots are denoted by z_2, z_3, etc. Because of the decreasing character of the envelope function the integral from z_1 to z_3 will be positive. It is useful to define a period of the function $G(z, \lambda z)$ as an interval between two next to neighbouring roots, i.e. from z_1 to z_3, from z_3 to z_5 and so on. Then the full integral in (22) will be a sum of the negative integral from $z = 0$ to $z = z_1$ and a multitude of positive integrals over subsequent periods. In the case of sufficiently small transverse size of the tube ($mr_0 < 0.1$) the integrals over some finite number of first periods may be negative but thereupon they become and remain positive also.

For small z ($z \lesssim 20$) we make a direct integration of the function $G(z, \lambda z)$ over periods using 25 digits of precision in internal computations.

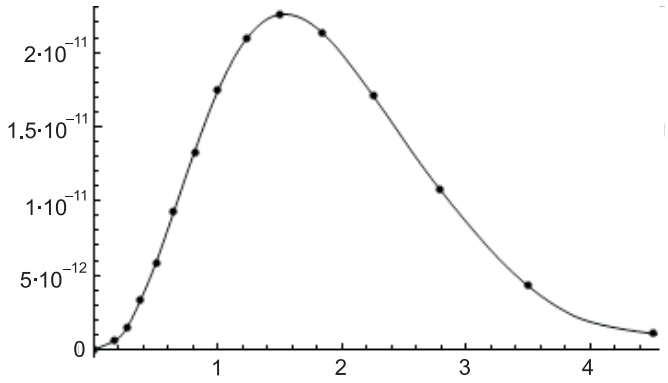

Figure 3. $r^3\varepsilon_{\rm ren}$ at $mr_0 = 3/2$ as a function of x.

For large z we make integration for each period separately. To carry this out we create a table of values of the function $G(z, \lambda z)$ for a separate period and replace this function by a more simple function in the form

$$G_{\rm int}(z, \lambda z) = a\frac{{\rm e}^{-bz}}{z^c}\frac{A_q(z^2)}{B_q(z^2)}\sin(kz + j\ln z + \phi_0), \tag{27}$$

where the sine function ensures that roots of $G_{\rm int}(z, \lambda z)$ coincide with roots of $G(z, \lambda z)$; $A_q(y)$ and $B_q(y)$ are q-degree polynomials, q can be 3, 4 or 5; all unknown parameters can be found from an interpolation procedure. We allow a relative error of interpolation to be

$$\left|\frac{G_{\rm int}(z, \lambda z) - G(z, \lambda z)}{G(z, \lambda z)}\right| < 10^{-8} \tag{28}$$

for each period. The function $G_{\rm int}(z, \lambda z)$ can be immediately integrated with the required accuracy. In this way we made integration up to $z \simeq 100/\lambda$ with an absolute accuracy up to 10^{-17}.

With the help of the above procedure we obtain a table of contributions from integration over each period, extrapolate this table to infinity and after that we find the full integral in (22) as a sum of the negative integral over first period(s), a multitude of positive integrals over periods up to $z \simeq 100/\lambda$ and an interpolation term. The absolute accuracy of the obtained result is 10^{-13}. It should be noted that nearly 99% of the integral value in (22) is obtained by direct calculation and only nearly 1% is the contribution from the interpolation.

The dimensionless quantity $r^3\varepsilon_{\rm ren}$ (22) is a function of two dimensionless parameters, mr_0 and mr. Using the above-described procedure, we calculate $r^3\varepsilon_{\rm ren}$ at several values of mr_0 as a function of the dimensionless distance from the edge of the vortex, $x = m(r - r_0)$, in the range $0 < x < 3mr_0$. Further increase of the distance from the vortex results in a significant increment of computational time, because there the envelope of $G(z, \lambda z)$ fails to be a sufficiently decreasing function as it is at smaller distances. The results of our numerical calculations are presented in figures 3–7, where $r^3\varepsilon_{\rm ren}$ is along the ordinate axis and x is along the abscissa axis; solid lines are interpolating the dots that have been calculated.

The typical behaviour of $r^3\varepsilon_{\rm ren}$ is clearly illustrated in cases $mr_0 \geqslant 1$ by figures 3 and 4. The vacuum energy density is zero at the edge of the vortex (at $x = 0$), starts increasing by some power law x^α with $\alpha > 1$, reaches maximum at $x \sim 1$ and decreases at larger distances to zero (probably exponentially as ${\rm e}^{-x}$). However, as mr_0 decreases, the available range of x is

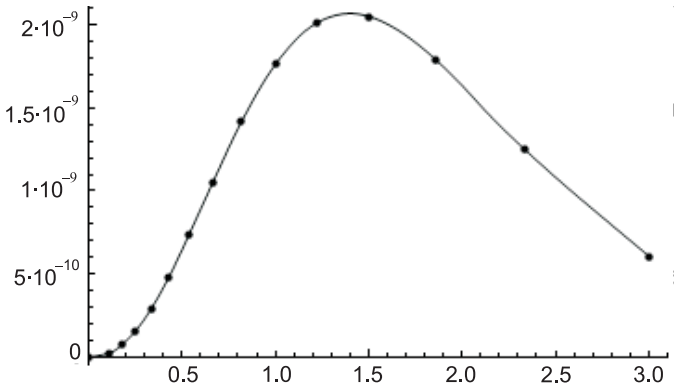

Figure 4. $r^3\varepsilon_{\rm ren}$ at $mr_0 = 1$ as a function of x.

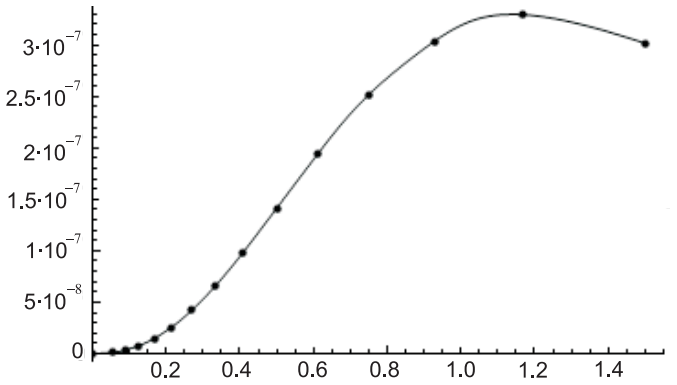

Figure 5. $r^3\varepsilon_{\rm ren}$ at $mr_0 = 1/2$ as a function of x.

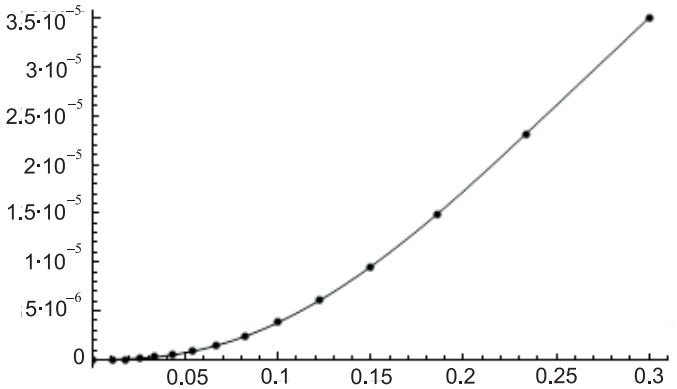

Figure 6. $r^3\varepsilon_{\rm ren}$ at $mr_0 = 10^{-1}$ as a function of x.

shrunk due to above-mentioned restriction $x < 3mr_0$. In the case of $mr_0 = 1/2$ a maximum at $x \sim 1$ is clearly seen (figure 5), and a following decrease to zero may be anticipated. In the

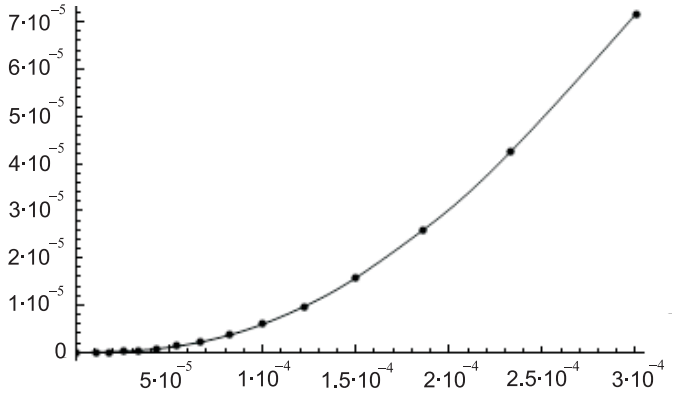

Figure 7. $r^3\varepsilon_{\rm ren}$ at $mr_0 = 10^{-4}$ as a function of x.

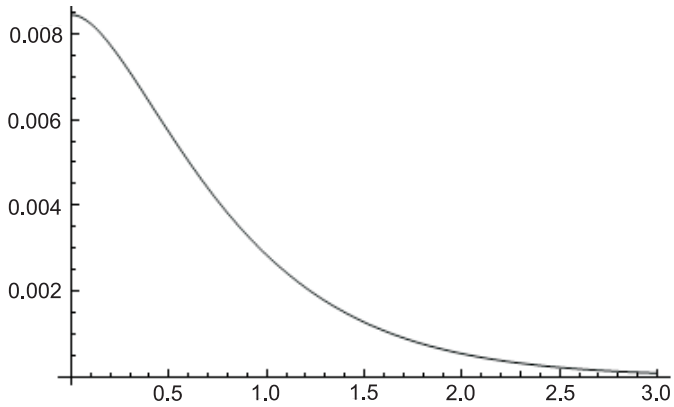

Figure 8. $r^3\varepsilon_{\rm ren}$ at $r_0 = 0$ as a function of mr.

cases of $mr_0 = 10^{-1}$ (figure 6) and $mr_0 = 10^{-4}$ (figure 7) one may suppose that there will be a maximum at $x \sim 1$ and a following decrease to zero. But, one can be sure for certain from figures 3–7 that the vacuum energy density decreases to zero as x^α with $\alpha > 1$ at $x \to 0$.

As to values of the vacuum energy density, they are rapidly decreasing as the parameter mr_0 increases and becomes more than unity. Namely, the maximal values of $r^3\varepsilon_{\rm ren}$ are 3.3×10^{-7} at $mr_0 = 1/2$ (figure 5), 2.1×10^{-9} at $mr_0 = 1$ (figure 4) and 2.2×10^{-11} at $mr_0 = 3/2$ (figure 3). These should be compared with much larger values which are already attained below maxima in figures 6 and 7: 3.5×10^{-5} at $mr_0 = 10^{-1}$ and 7×10^{-5} at $mr_0 = 10^{-4}$. It should be noted that, in the case of the singular vortex ($mr_0 = 0$), the maximal value of $r^3\varepsilon_{\rm ren}$ is $(12\pi^2)^{-1} \approx 8.5 \times 10^{-3}$ [9]; the appropriate plot of $r^3\varepsilon_{\rm ren}$ as a function of mr is taken from [11] and is presented in figure 8. Thus, one may suppose that, in the case of the vortex with thickness in the range $0 < mr_0 < 10^{-4}$, the maximal value of $r^3\varepsilon_{\rm ren}$ will be somewhere in the range 10^{-4}–10^{-3}. For more clarity, the results of figures 6 and 7 are plotted as functions of variable $r/r_0 = \lambda^{-1}$ in figure 9. Note that, as mr_0 falls by three orders from 10^{-1} to 10^{-4}, quantity $r^3\varepsilon_{\rm ren}$ changes by factor 2 only. This should be compared with $r^3\varepsilon_{\rm ren}$ at $m = 0$, which is plotted as a function of r/r_0 in figure 10; the latter plot coincides actually with that corresponding to $mr_0 = 10^{-4}$ in figure 9. It should be noted also that at sufficiently small

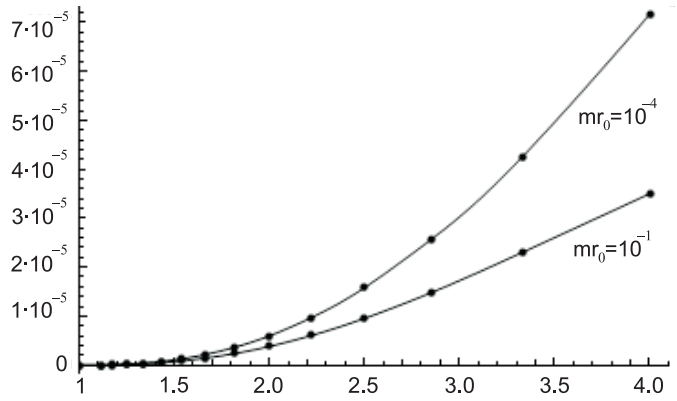

Figure 9. $r^3\varepsilon_{\rm ren}$ at the smallest values of mr_0 as a function of r/r_0.

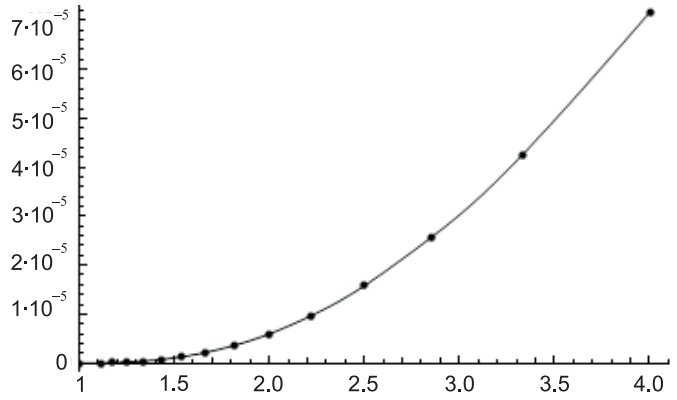

Figure 10. $r^3\varepsilon_{\rm ren}$ at $m = 0$ as a function of r/r_0.

distances from the vortex edge (at $r - r_0 \ll m^{-1}$) the behaviour of $r^3\varepsilon_{\rm ren}$ coincides with that in the $m = 0$ case.

4. Discussion of the results

We have studied the influence of finite thickness of the impenetrable magnetic vortex on the vacuum polarization of the quantized charged massive scalar field. Since units $c = \hbar = 1$ are used, the London flux value is $2\pi e^{-1}$, and we show that induced vacuum energy density (9) is periodic in the value of the vortex flux Φ, vanishing at integer multiples of the London flux value (at $\Phi = 2\pi n e^{-1}$) and being presumably maximal at half of the London flux value (at $\Phi = \pi(2n + 1)e^{-1}$). If the vortex thickness decreases, $r_0 \to 0$, or a distance from the vortex increases, $r - r_0 \to \infty$, then the contribution of $S_1(kr, kr_0)$ (14) and $\tilde{S}_1(kr, kr_0)$ (17) to (9) tends smoothly to zero, and the vacuum energy density converges with that induced by the singular magnetic vortex.

Our numerical analysis of the vortex thickness effects has been carried out for the case of the vortex flux equal to half of the London flux value; the quantized scalar field is confined to a plane which is orthogonal to the vortex. As follows from this analysis, the vacuum

polarization actually disappears, when the transverse size of the vortex (r_0) exceeds the Compton wavelength of the scalar particle (m^{-1}): the maximal value of the induced vacuum energy density falls by two orders from $2.6 \times 10^{-10} m^3$ to $1.4 \times 10^{-12} m^3$ as mr_0 increases from 1 to 3/2.

This result should be compared with the influence of the vortex thickness on the conventional Bohm–Aharonov effect. In the framework of first-quantized theory, one considers elastic scattering of a quantum-mechanical charged particle on the impenetrable magnetic vortex of thickness $2r_0$. The incident wave is characterized by momentum p, so the dimensionless parameter of the problem is pr_0. In the long-wavelength limit, $pr_0 \to 0$, scattering converges with scattering on the singular magnetic vortex [8]. Since the short-wavelength limit, $pr_0 \to \infty$, corresponds to the case when quasi-classical approximation is applicable, one would anticipate that the purely quantum effect, as is the Bohm–Aharonov one, disappears in this limit. As it has been shown in [7], this anticipation is indeed confirmed, and scattering in the $pr_0 \to \infty$ limit converges with scattering of a classical point particle on the impenetrable tube, being independent of the enclosed magnetic flux.

In the framework of second-quantized theory, one considers the vacuum polarization in the background of the impenetrable magnetic vortex. The appropriate dimensionless parameter is mr_0, and, as we have shown in the present paper, the Casimir–Bohm–Aharonov effect disappears in the $mr_0 \to \infty$ limit becoming actually negligible at $mr_0 > 3/2$.

In the case of the singular magnetic vortex, the induced vacuum energy density diverges at the location of the vortex [6, 9–11]. As it has been shown in the present paper, this divergence is unphysical, disappearing when thickness of the impenetrable magnetic vortex is taken into account: under the Dirichlet condition for the quantized field (4), the induced vacuum energy density is vanishing as $(r - r_0)^\alpha$ with $\alpha > 1$ at the edge of the vortex. Therefore, the vacuum energy which is induced on the whole transverse plane,

$$E_{\mathrm{ren}} = 2\pi \int_{r_0}^{\infty} \mathrm{d}r\, r \varepsilon_{\mathrm{ren}}, \tag{29}$$

is finite, contrary to the case of the singular vortex when it is infinite. Although we are unaware of the value of E_{ren}, the maximal value of $\varepsilon_{\mathrm{ren}}$ is estimated to be somewhat of the order of $10^{-3} m^3$ if $mr_0 < 10^{-4}$.

A brief discussion of polarization of the vacuum of the quantized massless scalar field is in order. In this case, the induced vacuum energy density is zero at the edge of the vortex, starts increasing as $(r - r_0)^\alpha$ with $\alpha > 1$ (see figure 10), reaches its maximum and then decreases with asymptotics $(12\pi^2 r^3)^{-1}$ [9–11]. Induced vacuum energy (29) is finite in this case also.

The finite-thickness vortex can be formed as a topological defect appearing after a phase transition with spontaneous breakdown of the gauge symmetry [19]. Such a structure under the name of a cosmic string [20, 21] is currently discussed in various contexts in cosmology and astrophysics, see, e.g., [22, 23]. The cosmic string is characterized by the flux $2\pi e_{\mathrm{H}}^{-1}$, where e_{H} is the coupling constant of the Higgs scalar field to the string-forming gauge field; the transverse size of the string is of the order of correlation length m_{H}^{-1}, where m_{H} is the mass of the Higgs scalar field. Then, as it follows from our consideration in the present paper, the cosmic string can polarize the vacuum of quantum matter only in the case when the mass of the matter field is much less than that of the Higgs field, $m \ll m_{\mathrm{H}}$. For instance, the cosmic string which is formed at the grand unification scale can polarize the vacuum of the electroweak theory, whereas the would-be cosmic string corresponding to the electroweak symmetry breaking has no impact on the vacuum of quantum matter at the grand unification scale.

Acknowledgments

YAS acknowledges the support from the State Foundation for Fundamental Research under project F28.2/083 'Application of the string theory and the field theory methods to the study of nonlinear phenomena in low-dimensional systems' and from the National Academy of Science of Ukraine under project 10/07-N 'Study of physical properties of nanomaterials for electronics, photonics, spintronics and information technologies'.

References

[1] Casimir H B G 1948 *Proc. Kon. Ned. Akad. Wetenschap* B **51** 793
Casimir H B G 1953 *Physica* **19** 846
[2] Elizalde E 1995 *Ten Physical Applications of Spectral Zeta Functions* (Berlin: Springer)
[3] Mostepanenko V M and Trunov N N 1997 *The Casimir Effect and Its Applications* (Oxford: Clarendon)
[4] Bordag M, Mohideen U and Mostepanenko V M 2001 *Phys. Rep.* **353** 1
[5] Aharonov Y and Bohm D 1959 *Phys. Rev.* **115** 485
[6] Sitenko Yu A and Babansky A Yu 1998 *Mod. Phys. Lett.* A **13** 379
[7] Olariu S and Iovitzu Popescu I 1985 *Rev. Mod. Phys.* **57** 339
[8] Skarzhinsky V D 1986 *Trudy FIAN Proc. Lebedev. Inst.* **167** 139 (In Russian)
[9] Sitenko Yu A and Babansky A Yu 1998 *Phys. Atom. Nucl.* **61** 1594
[10] Sitenko Yu A and Gorkavenko V M 2003 *Ukrainian J. Phys.* **48** 1286
[11] Sitenko Yu A and Gorkavenko V M 2003 *Phys. Rev.* D **67** 085015
[12] Fry M P 1996 *Phys. Rev.* D **54** 6444
[13] Dunne G and Hall T M 1998 *Phys. Lett.* B **419** 322
[14] Bordag M and Kirsten K 1999 *Phys. Rev.* D **60** 105019
[15] Langfeld K, Moyaerts L and Gies H 2002 *Nucl. Phys.* B **646** 158
[16] Graham N, Khemani V, Quandt M, Schroeder O and Weigel H 2005 *Nucl. Phys.* B **707** 233
[17] Babansky A Yu and Sitenko Yu A 1999 *Theor. Math. Phys.* **120** 876
[18] Wirzba A 2008 *J. Phys. A: Math. Theor.* **41** 164003
[19] Abrikosov A A 1957 *Sov. Phys.—JETP* **5** 1174
[20] Vilenkin A and Shellard E P S 1994 *Cosmic Strings and Other Topological Defects* (Cambridge: Cambridge University Press)
[21] Hindmarsh M B and Kibble T W B 1995 *Rep. Prog. Phys.* **58** 477
[22] Polchinski J 2005 *Int. J. Mod. Phys.* A **20** 3413
[23] Sazhin M V, Khovanskaya O S, Capaccioli M, Longo L, Paolillo M, Covone G, Grogin N A and Schreier E J 2007 *Mon. Not. R. Astron. Soc.* **376** 1731